Oxidative Addition of Trisubstituted Silanes to Photochemically Generated Coordinatively Unsaturated Species $(\eta^4\text{-}C_4H_4)Fe(CO)_2$, $(\eta^5\text{-}C_5H_5)Mn(CO)_2$, and $(\eta^6\text{-}C_6H_6)Cr(CO)_2$ and Related Molecules

Ross H. Hill and Mark S. Wrighton*

Department of Chemistry, Massachusetts Institute of Technology, Cambridge, Massachusetts 02139

Received June 20, 1986

Irradiation of $(\eta^4\text{-}C_4H_4)Fe(CO)_3$, $(\eta^5\text{-}C_5H_5)Mn(CO)_3$, $(\eta^5\text{-}C_5Me_5)Mn(CO)_3$, $(\eta^5\text{-}C_5H_5)Re(CO)_3$, and $(\eta^6\text{-}C_6H_6)Cr(CO)_3$ leads to dissociative CO loss to form 16e dicarbonyl species. At low temperatures, 85–157 K, the unsaturated dicarbonyl molecules can be spectroscopically (IR) characterized in inert organic solvents, such as methylcyclohexane or 3-methylpentane. In the presence of R_3SiH the dicarbonyl species react to form 18e oxidative addition products of the formula $(\eta^n\text{-}C_nR_n)MH(SiR_3)(CO)_2$. For all dicarbonyl species the rate of reaction with Et_3SiH was investigated. For the Fe and two Mn species a complete study of rate vs. temperature was made. The Cr species reacts too fast to measure quantitatively. The reaction of Et_3SiH with the Re species occurs only above 157 K, and detailed studies were not made. The results give an overall reactivity trend for the dicarbonyls toward neat Et_3SiH at 100 K of Cr > Mn > Fe > Re and $C_5Me_5 > C_5H_5$. The difference in rate with C_5Me_5 vs. C_5H_5 is a factor of $\sim 10^2$ over a wide temperature range, and the difference between Cr and Re at 100 K is at least 10^4. The reactivities of various silanes toward $(\eta^5\text{-}C_5H_5)Mn(CO)_2$ were also investigated as a function of temperature. The activation parameters, $\Delta H^\ddagger$ and $\Delta S^\ddagger$, show only modest variation with silane such that $\Delta H^\ddagger$ $EtMe_2SiH$ (25 ± 1 kJ mol^{-1}) < Ph_3SiH (28 ± 1 kJ mol^{-1}) < $i\text{-}Pr_3SiH$ (29 ± 1 kJ mol^{-1}) < $n\text{-}Pr_3SiH$ (30 ± 1 kJ mol^{-1}) ≈ Et_3SiH (30 ± 1 kJ mol^{-1}) and $\Delta S^\ddagger$ Et_3SiH (−28 ± 5 J K^{-1} mol^{-1}) < $n\text{-}Pr_3SiH$ (−31 ± 5 J K^{-1} mol^{-1}) ≈ Ph_3SiH (−31 ± 5 J K^{-1} mol^{-1}) < $i\text{-}Pr_3SiH$ (−33 ± 5 J K^{-1} mol^{-1}) < $EtMe_2SiH$ (−40 ± 5 J K^{-1} mol^{-1}).

We wish to report the results of a study of the thermal reactivity of trisubstituted silanes with the d^6 16e complexes produced at low temperature by near-UV irradiation of $(\eta^4\text{-}C_4H_4)Fe(CO)_3$, $(\eta^5\text{-}C_5H_5)Mn(CO)_3$, $(\eta^5\text{-}C_5Me_5)Mn(CO)_3$, $(\eta^5\text{-}C_5H_5)Re(CO)_3$, and $(\eta^6\text{-}C_6H_6)Cr(CO)_3$ (eq 1 and 2). Back reaction of the 16e species with CO is possible

$$(\eta^n\text{-}C_nR_n)M(CO)_3 \xrightarrow{h\nu} (\eta^n\text{-}C_nR_n)M(CO)_2 + CO \quad (1)$$

$$(\eta^n\text{-}C_nR_n)M(CO)_2 + R_3SiH \rightarrow (\eta^n\text{-}C_nR_n)MH(SiR_3)(CO)_2 \quad (2)$$

(eq 3). There are several reports in the literature con-

$$(\eta^n\text{-}C_nR_n)M(CO)_2 + CO \rightarrow (\eta^n\text{-}C_nR_n)M(CO)_3 \quad (3)$$

cerning the kinetics and mechanism of oxidative addition to coordinatively unsaturated d^8 complexes.[1] Studies of d^6 systems are generally hampered by the fact that the rate-limiting step is dissociation of a ligand because the d^6 systems are typically found as 18e species. For example, ligand substitution reactions of d^6 metal carbonyls are largely dissociative.[2] Thus, kinetic analysis of oxidative addition processes generally yields information only for the rate-limiting ligand dissociation. The oxidative addition chemistry of d^6 systems is important in catalytic[3] and stoichiometric processes including C–H activation by $(\eta^5\text{-}C_5H_5)Re(CO)PMe_3$.[4] In view of the generality of oxidative addition to d^6 systems and the lack of kinetic information about such systems, we have undertaken this study to learn the effect on oxidative addition rates resulting from systematic changes in both the metal complex and the silane.

In order to obtain quantitative data regarding oxidative addition rates to 16e d^6 systems, it is necessary to be able to generate and quantitatively monitor the concentration of the desired 16e coordinatively unsaturated fragments. There are many reports in the literature of the observation of d^6 coordinatively unsaturated species produced by light-induced CO loss at low temperature.[5,6] We chose to study the series of arene metal dicarbonyls for two reasons. First, oxidative addition of the trisubstituted silane to $(\eta^5\text{-}C_5H_5)Mn(CO)_2$, $(\eta^5\text{-}C_5Me_5)Mn(CO)_2$, $(\eta^5\text{-}C_5H_5)Re(CO)_2$, and $(\eta^6\text{-}C_6H_6)Cr(CO)_2$ has been established to result from irradiation of the tricarbonyl species[7] in solution. Second, photochemical dissociation of CO from $(\eta^4\text{-}C_4H_4)Fe(CO)_3$, $(\eta^5\text{-}C_5H_5)Mn(CO)_3$, and $(\eta^6\text{-}C_6H_6)Cr(CO)_3$ at low temperatures has been reported.[8,9] Since the dissociation of CO can be induced at temperatures as low as 12 K, we felt it would be possible to choose a temperature such that the photochemical reaction, CO dissociation (eq 1), could be induced at a rate faster than the thermal oxidative addition (eq 2). Under conditions where the reaction of eq 1 proceeds faster that the reaction of eq 2, the arene metal dicarbonyl accumulates, provided back reaction with the photogenerated CO (eq 3) is too slow to compete for the dicarbonyl. Hence, the rate of reaction according to eq 2 can be directly measured.

The reaction of the full series of arene metal dicarbonyls with Et_3SiH has been investigated. For $(\eta^5\text{-}C_5H_5)Mn(CO)_2$ a more complete study was undertaken, and the activation parameters $\Delta H^\ddagger$ and $\Delta S^\ddagger$ have been obtained for reaction

(1) Mondal, J. U.; Blake, D. M. *Coord. Chem. Rev.* **1982**, *47*, 205.
(2) Howell, J. A. S.; Burkinshaw, P. M. *Chem. Rev.* **1983**, *83*, 557.
(3) Masters, C. *Homogeneous Transition Metal Catalysis*; Chapman Hall: London, 1981.
(4) Bergman, R. G.; Seidler, P. F.; Wenzel, T. T. *J. Am. Chem. Soc.* **1985**, *107*, 4358.
(5) Blaha, J. P.; Wrighton, M. S. *J. Am. Chem. Soc.* **1985**, *107*, 2694.
(6) Pope, K. R.; Wrighton, M. S. *Inorg. Chem.* **1985**, *24*, 2792.
(7) (a) Jetz, W.; Graham, W. A. G. *Inorg. Chem.* **1971**, *10*, 4. (b) Hoyano, J. K.; Graham, W. A. G. *Organometallics* **1982**, *1*, 783. (c) Dong, D. F.; Hoyano, J. K.; Graham, W. A. G. *Can. J. Chem.* **1981**, *59*, 1455. (d) Graham, W. A. G. *J. Organomet. Chem.* **1986**, *300*, 81.
(8) Chapman, O. L.; Palansky, J.; Wojtkowski, P. J. *J. Chem. Soc., Chem. Commun.* **1973**, 681.
(9) Rest, A. J.; Sodeau, J. R.; Taylor, D. J. *J. Chem. Soc., Dalton Trans.* **1978**, 651.

0276-7333/87/2306-0632$01.50/0

with the series of silanes of differing steric bulk, i-Pr_3SiH, n-Pr_3SiH, Et_3SiH, $EtMe_2SiH$, and Ph_3SiH. A communication of work on the $(\eta^4\text{-}C_4H_4)Fe(CO)_2/Et_3SiH$ system has appeared.[10]

Experimental Section

Instruments. Infrared spectral data were recorded by using a Nicolet 60SX or 7199 FTIR spectrometer. ^1H NMR spectra were recorded by using a Varian T-60 or a Bruker 250 NMR spectrometer. Chemical shifts are referred to Me_4Si. Irradiations were carried out by using the H_2O-filtered output from a Baush and Lomb SP200 200-W high-pressure Hg lamp.

Low-temperature FTIR experiments were done in CaF_2-faced cells in either a Specac Model P/N 21 000 Dewar assembly or in a C.T.I. Cyrogenics/Spectrim Model 21 variable-temperature system. In each case the temperature was monitored by use of a thermocouple, and the cell mount was heated to maintain constant temperature.

Chemicals. The methylcyclohexane and 3-methylpentane were spectroquality solvents obtained commercially. The metal carbonyl complexes $BrRe(CO)_5$, $(\eta^4\text{-}C_4H_4)Fe(CO)_3$, $(\eta^5\text{-}C_5H_5)Mn(CO)_3$, $(\eta^5\text{-}C_5Me_5)Mn(CO)_3$, and $(\eta^6\text{-}C_6H_6)Cr(CO)_3$ were purchased from Strem Chemicals. The silanes Et_3SiH, n-Pr_3SiH, i-Pr_3SiH, Ph_3SiH, and $EtMe_2SiH$ were obtained from Petrarch Systems, Inc. $(\eta^5\text{-}C_5H_5)Re(CO)_3$ was prepared by a literature procedure[11] and recrystallized from hexane. The complexes $(\eta^6\text{-}C_6H_5Me)Cr(CO)_3$, $(\eta^6\text{-}C_6H_5Et)Cr(CO)_3$, and $(\eta^6\text{-}C_6H_5Bu)Cr(CO)_3$ were prepared by published procedures.[12]

Characterization of the Silane Adducts. A sample of $(\eta^4\text{-}C_4H_4)Fe(CO)_3$ (0.02 g) was dissolved in 1-mL solution containing 30% (v/v) Et_3SiH in methylcyclohexane-d_{14}. This solution was purged with Ar in a 5-mm NMR tube and irradiated with a high-pressure Hg lamp for 15 min while immersed in a dry ice/acetone bath. The NMR tube was then transferred to the cooled probe (−70 °C) of the Bruker 250. The NMR obtained showed the presence of a resonance due to the Fe–H at −11.0 ppm, and a signal due to $(\eta^4\text{-}C_4H_4)$ at 4.0 ppm. The $(\eta^5\text{-}C_5H_5)MnH(SiR_3)(CO)_2$ type complexes are well-known for a variety of R groups, and the complex with R = Ph has been crystallographically characterized.[15] The new derivatives were characterized by IR (Table I) and NMR data: R = Et, $\delta(\eta\text{-}C_5H_5)$ 4.4, δ(MnH) −13.8; R = i-Pr, $\delta(\eta\text{-}C_5H_5)$ 4.2, δ(MnH) −15.1; R = n-Pr, $\delta(\eta\text{-}C_5H_5)$ 4.45, δ(MnH) −13.2; R_3 = $EtMe_2$, $\delta(\eta\text{-}C_5H_5)$ 4.5, δ(MnH) −10.8; $(\eta\text{-}C_5Me_5)MnH(SiEt_3)(CO)_2$, $\delta(\eta\text{-}C_5Me_5)$ ~1.9 (not resolved from tricarbonyl species), δ(MnH) −13.7.

The $(\eta^5\text{-}C_5H_5)ReH(SiEt_3)(CO)_2$ is a known compound.[7] The $(\eta^6\text{-}C_6H_6)CrH(SiEt_3)(CO)_2$ was characterized by its IR (Table I) and ^1H NMR data [$\delta(\eta^6\text{-}C_6H_6)$ 4.2, δ(Cr–H) −14.9] and by comparison with other known silane adducts.[7]

Extinction coefficients for starting tricarbonyls were determined at 298 K, and extinction coefficient for oxidative addition products were determined assuming quantitative conversion of the tricarbonyl to the dicarbonyl species. ^1H NMR studies show such an assumption to be valid within 5%.

Kinetic Measurements. A typical kinetic measurement was done in the following way. A Et_3SiH solution of $(\eta^5\text{-}C_5H_5)Mn(CO)_3$ (1.4×10^{-4} M) was loaded into a 0.2 mm path length CaF_2 IR cell and cooled to 111 K. The sample was then photolyzed such that 15% of the $(\eta^5\text{-}C_5H_5)Mn(CO)_3$ had been removed and $(\eta^5\text{-}C_5H_5)Mn(CO)_2$ was detected by FTIR. FTIR spectra were then recorded as a function of time in the dark to quantitatively monitor growth of $(\eta^5\text{-}C_5H_5)MnH(SiEt_3)(CO)_2$ and decline of $(\eta^5\text{-}C_5H_5)Mn(CO)_2$. Care was taken to ensure that the IR beam of the spectrometer does not accelerate the "dark" reactions between the 16e species and silane. Control experiments show no beam-induced chemistry on the time scale of data acquisition. Regeneration of $(\eta^5\text{-}C_5H_5)Mn(CO)_3$ could also be detected in some cases, but the amount of CO back reaction was typically a minor process for the Mn complexes under the conditions used. A typical competition experiment to determine relative silane reactivity was run as follows: a 3-methylpentane solution containing $(\eta^5\text{-}C_5H_5)Mn(CO)_3$ (~6×10^{-4} M), Et_3SiH (1.58×10^{-3} mol), and Ph_3SiH (9.5×10^{-4} mol) was prepared and introduced into a 0.1-mm IR cell. This solution was then photolyzed with the output of a Xenon Corp. flash photolysis apparatus utilizing two FP5-100c xenon flash tubes charged to 5 kV yielding a 20-μs light pulse. The conversion to $(\eta^5\text{-}C_5H_5)MnH(SiEt_3)(CO)_2$ and $(\eta^5\text{-}C_5H_5)MnH(SiPh_3)(CO)_2$ was monitored by FTIR and the relative amounts produced found to be 3.8/4.7. Solving for relative rate constants gives k(reaction with Ph_3SiH)/k(reaction with Et_3SiH) = 2.0 ± 0.04.

Table I. Spectroscopic Data for Relevant Compounds[a]

complex	T, K	ν(CO), ± 2 cm^{-1} (ε, M^{-1} cm^{-1}, or rel abs)
$(\eta^4\text{-}C_4H_4)Fe(CO)_3$	298	1980 (10 700), 2052 (5400)
	100	1972 (7900), 1980 (7700), 2050 (7000)
$(\eta^4\text{-}C_4H_4)Fe(CO)_2$	100	1923 (1.4), 1991 (1.0)
	12	1936,[c] 2005[c]
$(\eta^4\text{-}C_4H_4)FeH(SiEt_3)(CO)_2$	100	1950 (1.0), 2010 (1.0)
$(\eta^5\text{-}C_5H_5)Mn(CO)_3$	298	1947 (12 700), 2028 (5700)
	100	1942 (12 300), 2027 (9100)
$(\eta^5\text{-}C_5H_5)Mn(CO)_2$	100	1880 (1.1), 1950 (1.0)
	12	1903,[c] 1972[c]
$(\eta^5\text{-}C_5H_5)MnH(SiEt_3)(CO)_2$	298	1914 (2700), 1977 (3100)[b]
	100	1910 (1.1), 1975 (1.0)[b]
$(\eta^5\text{-}C_5H_5)MnH(SiMe_2Et)(CO)_2$	298	1918 (2500), 1980 (2800)
$(\eta^5\text{-}C_5H_5)MnH(Si\text{-}i\text{-}Pr_3)(CO)_2)$	298	1905 (2000, 1966 (2000)
$(\eta^5\text{-}C_5H_5)MnH(Si\text{-}n\text{-}Pr_3)(CO)_2$	298	1915 (3100), 1977 (3300)
$(\eta^5\text{-}C_5H_5)MnH(SiPh_3)(CO)_2$	298	1929 (1700), 1985 (2500)
$(\eta^5\text{-}C_5Me_5)Mn(CO)_3$	298	1927 (12 400), 2009 (6700)
	100	1923 (13 300), 2008 (7000)
$(\eta^5\text{-}C_5Me_5)Mn(CO)_2$	100	1863 (1.0), 1932 (1.2)
$(\eta^5\text{-}C_5Me_5)MnH(SiEt_3)(CO)_2$	298	1888 (1.0), 1948 (1.0)[b]
	100	1890 (1.0), 1944 (1.1)[b]
$(\eta^5\text{-}C_5H_5)Re(CO)_3$	298	1934 (16 200), 2031 (5900)
	100	1934 (13 200), 2028 (5300)
$(\eta^5\text{-}C_5H_5)Re(CO)_2$	100	1879 (1.5), 1946 (1.0)
$(\eta^5\text{-}C_5H_5)ReH(SiEt_3)(CO)_2$	298	1918 (6200), 1990 (5900)[b]
$(\eta^6\text{-}C_6H_6)Cr(CO)_3$	298	1917 (12 700), 1984 (11 500)
$(\eta^6\text{-}C_6H_6)Cr(CO)_2$	12	1885,[c] 1937[c]
$(\eta^6\text{-}C_6H_6)CrH(SiEt_3)(CO)_2$	100	1821 (1.0), 1921 (1.2)[b]

[a] In methylcyclohexane solvent unless otherwise noted. [b] In $HSiEt_3$. [c] In Ar; from ref 9.

Results

Photogeneration of $(\eta^n\text{-}C_nR_n)M(CO)_2$ and Oxidative Addition Products. Generally, photolysis of $(\eta^n\text{-}C_nR_n)M(CO)_3$ species in a hydrocarbon glass at ~100 K leads to loss of IR absorption due to the starting complexes and growth of new peaks associated with free CO and the unsaturated $(\eta^n\text{-}C_nR_n)M(CO)_2$ species. For instance, at 100 K in methylcyclohexane peaks due to $(\eta^5\text{-}C_5H_5)Mn(CO)_3$ at 2027 and 1942 cm^{-1} decrease in intensity accompanied by growth of peaks due to free CO at 2132 cm^{-1} and the dicarbonyl species $(\eta^5\text{-}C_5H_5)Mn(CO)_2$ at 1950 and 1880 cm^{-1} (Figure 1b). The stoichiometry of CO loss from $(\eta^5\text{-}C_5H_5)Mn(CO)_3$ can be determined knowing the extinction coefficients for CO ($\epsilon \approx 400$ M^{-1} cm^{-1})[6] and (η^5-

(10) Hill, R. H.; Wrighton, M. S. *Organometallics* **1985**, *4*, 413.
(11) Fischer, E. O.; Fellman, W. *J. Organomet. Chem.* **1963**, *1*, 191.
(12) Jackson, W. R.; Jenning, W. B.; Rennison, S. C.; Spratt, R. *J. Chem. Soc.* B **1969**, 1212.
(13) Sandstrom, J. *Dynamic NMR Spectroscopy*; Academic: New York, 1982.
(14) Based on arguments similar to those in: Cotton, F. A.; Kraihanzel, C. S. *J. Am. Chem. Soc.* **1962**, *84*, 4432.
(15) (a) Carre, F.; Colomer, E.; Corriu, R. J. P.; Vioux, A. *Organometallics* **1984**, *3*, 1272 and references cited therein. (b) Hutcheon, W. L. Ph.D. Thesis, University of Alberta, 1971 (as quoted in ref 7d). (c) Schubert, U.; Scholz, G.; Muller, J.; Ackermann, K.; Worle, B.; Stansfield, R. F. D. *J. Organomet. Chem.* **1986**, *306*, 303.

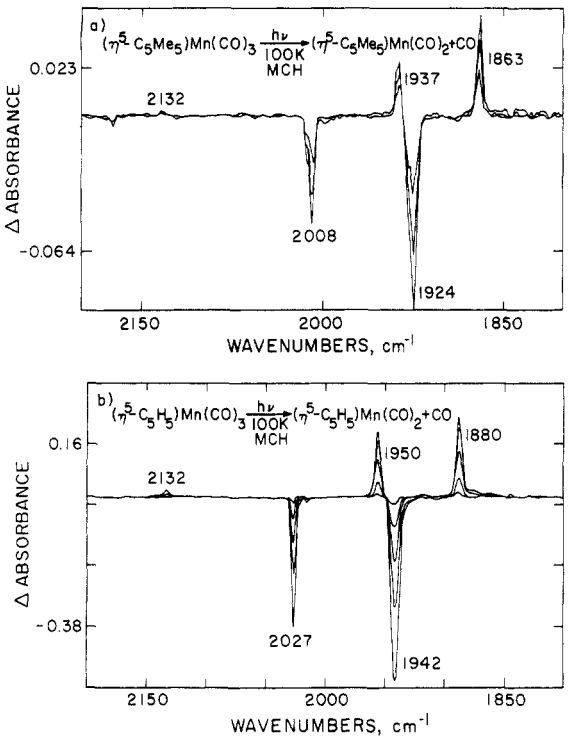

Figure 1. IR difference spectral changes accompanying near-UV irradiation of (a) $(\eta^5\text{-}C_5Me_5)Mn(CO)_3$ and (b) $(\eta^5\text{-}C_5H_5)Mn(CO)_3$ at 100 K in methylcyclohexane. Negative peaks correspond to consumption of the tricarbonyl, and positive peaks correspond to dicarbonyl photoproduct.

$C_5H_5)Mn(CO)_3$ in a low-temperature matrix. From the quantitative measurement of increase in CO absorption[6] and decrease in absorption due to $(\eta^5\text{-}C_5H_5)Mn(CO)_3$, we measure a net loss of one CO molecule for each molecule of $(\eta^5\text{-}C_5H_5)Mn(CO)_3$ consumed (eq 4). For $(\eta^5\text{-}C_5Me_5)$-

$$(\eta^5\text{-}C_5H_5)Mn(CO)_3 \xrightarrow{h\nu} (\eta^5\text{-}C_5H_5)Mn(CO)_2 + CO \quad (4)$$

$Mn(CO)_3$ in methylcyclohexane near-UV photolysis also results in CO loss. Figure 1a illustrates the FTIR spectral changes associated with loss of starting material at 2008 and 1924 cm^{-1} and growth of absorption due to formation of free CO at 2132 cm^{-1} and the 16e species $(\eta^5\text{-}C_5Me_5)$-$Mn(CO)_2$ at 1937 and 1863 cm^{-1}. Once again CO loss can be quantitated, and the stoichiometry is one mole of CO formed per mole of $(\eta^5\text{-}C_5Me_5)Mn(CO)_3$ consumed. Similar results are obtained with the $(\eta^4\text{-}C_4H_4)Fe(CO)_3$ and $(\eta^5\text{-}C_5H_5)Re(CO)_3$ systems, and the relevant band positions are given in Table I. The absorptivity of CO in the alkane glass is much lower than the absorptivity of the $(\eta^n\text{-}C_nR_n)M(CO)_3$ species studied. This causes difficulties in determining the stoichiometry for loss of CO, and we estimate that the data yield the conclusion that 1.0 ± 0.2 CO's appear for each $(\eta^n\text{-}C_nR_n)M(CO)_3$ consumed. However, it should be noted that photoproducts other than $(\eta^n\text{-}C_nR_n)M(CO)_2$ are not detected. We thus conclude that eq 1 represents the only net photochemistry of $(\eta^5\text{-}C_5R_5)Mn(CO)_3$ (R = H, Me), $(\eta^5\text{-}C_5H_5)Re(CO)_3$, and $(\eta^4\text{-}C_4H_4)Fe(CO)_3$.

In contrast to results for $(\eta^4\text{-}C_4H_4)Fe(CO)_3$, $(\eta^5\text{-}C_5R_5)$-$Mn(CO)_3$ (R = H, Me), and $(\eta^5\text{-}C_5H_5)Re(CO)_3$, we have been unable to detect the CO loss product from irradiation of $(\eta^6\text{-}C_6H_6)Cr(CO)_3$ in alkane glasses at low temperatures. The Cr species precipitates from the alkane at low temperature, and IR spectra are severely complicated by aggregation. At temperatures (~100 K) where the CO stretching absorptions are sharp, no net photoreaction in pure alkane can be detected, presumably due to rapid back reaction of photoejected CO with $(\eta^6\text{-}C_6H_6)Cr(CO)_2$. At the low temperatures where CO back reaction would be slow the $(\eta^6\text{-}C_6H_6)Cr(CO)_3$ precipitates. Unfortunately, the substituted complexes $(\eta^6\text{-}C_6H_5R)Cr(CO)_3$ (R = Me, Et, *n*-Bu) behave in the same manner. However, in Ar matrices photoconversion of $(\eta^6\text{-}C_6H_6)Cr(CO)_3$ to $(\eta^6\text{-}C_6H_6)$-$Cr(CO)_2$ has been detected.[9]

Reaction according to eq 1 has been investigated previously in an Ar matrix[9] for the species $(\eta^4\text{-}C_4H_4)Fe(CO)_3$, $(\eta^5\text{-}C_5H_5)Mn(CO)_3$, and $(\eta^6\text{-}C_6H_6)Cr(CO)_3$. Included in Table I are the IR absorption frequencies observed for the unsaturated species in an Ar matrix. It is interesting to note that the average CO stretching frequencies observed for the dicarbonyl-unsaturated species are at lower energy in hydrocarbon glass (at ~100 K) than in Ar (at ~12 K). This shift toward lower energy may result from better solvation of the unsaturated species in a hydrocarbon glass.

Generation of $(\eta^n\text{-}C_nR_n)M(CO)_2$ in a glass containing R_3SiH followed by warming results in chemistry according to eq 2 in competition with back reaction (eq 3). In the absence of R_3SiH, warming the matrix containing the 16e species and CO gives only back reaction. For example, warming of solutions containing $(\eta^5\text{-}C_5H_5)Mn(CO)_2$ in the presence of Et_3SiH results in loss of IR absorption bands at 1950 and 1880 cm^{-1} due to the 16e species and the growth of two new absorption bands at 1975 and 1910 cm^{-1} attributed to formation of $(\eta^5\text{-}C_5H_5)MnH(SiEt_3)(CO)_2$ (eq 5). Further evidence for formation of the oxidative ad-

$$(\eta^5\text{-}C_5H_5)Mn(CO)_2 + HSiEt_3 \rightarrow (\eta^5\text{-}C_5H_5)MnH(SiEt_3)(CO)_2 \quad (5)$$

dition product was obtained by low-temperature ^1H NMR. Photolysis of $(\eta^5\text{-}C_5H_5)Mn(CO)_3$ in methylcyclohexane-d_{14} at 298 K containing Et_3SiH results in growth or IR absorptions at 1977 and 1914 cm^{-1} and appearance of a ^1H NMR resonance at −13.7 ppm consistent with formation of a Mn–H species. Similar spectroscopic results are obtained for reaction of R_3SiH with $(\eta^4\text{-}C_4H_4)Fe(CO)_2$, $(\eta^5$-$C_5Me_5)Mn(CO)_2$, and $(\eta^5\text{-}C_5H_5)Re(CO)_2$: IR changes show formation of the oxidative addition products that can be further characterized by IR and ^1H NMR, cf. Table I and Experimental Section. Low-temperature (~90 K) irradiation of $(\eta^6\text{-}C_6H_6)Cr(CO)_3$ in the presence of Et_3SiH leads to the prompt generation of $(\eta^6\text{-}C_6H_6)CrH(SiEt_3)(CO)_2$ without a detectable intermediate. With the exception of Fe and Cr the R_3SiH oxidative addition products are found to be relatively inert at room temperature in either pure R_3SiH solvent or alkane containing R_3SiH. Thus, the complexes could be generated and characterized at room temperature. Attempted isolation of the product complexes was not successful. For instance, photolysis of an air-free Et_3SiH solution of $(\eta^5\text{-}C_5H_5)Mn(CO)_3$ leads to the production of $(\eta^5\text{-}C_5H_5)MnH(SiEt_3)(CO)_2$ as identified by IR. Evaporation of solvent under N_2 gives a yellow solid, presumably $(\eta^5\text{-}C_5H_5)MnH(SiEt_3)(CO)_2$. Recovery of the solid in a N_2 glovebox by filtration results in decomposition of the solid. For $(\eta^6\text{-}C_6H_6)Cr(CO)_3$ photolysis at 196 K in the presence of Et_3SiH results in formation of $(\eta^6\text{-}C_6H_6)$-$CrH(SiEt_3)(CO)_2$. This reaction was monitored by both IR and ^1H NMR. The $(\eta^6\text{-}C_6H_6)CrH(SiEt_3)(CO)_2$ decomposes near room temperature. Similar results are obtained for $(\eta^4\text{-}C_4H_4)FeH(SiEt_3)(CO)_2$ that decomposes at 220 K.

The Kinetics of the Oxidative Addition of R_3SiH to $(\eta^n\text{-}C_nR_n)M(CO)_2$. The kinetics for reaction of $(\eta^n$-$C_nR_n)M(CO)_2$ according to eq 2 were investigated in the following way. A sample of the $(\eta^n\text{-}C_nR_n)M(CO)_3$ species in either neat R_3SiH or a hydrocarbon solution containing R_3SiH was prepared and loaded into a low-temperature

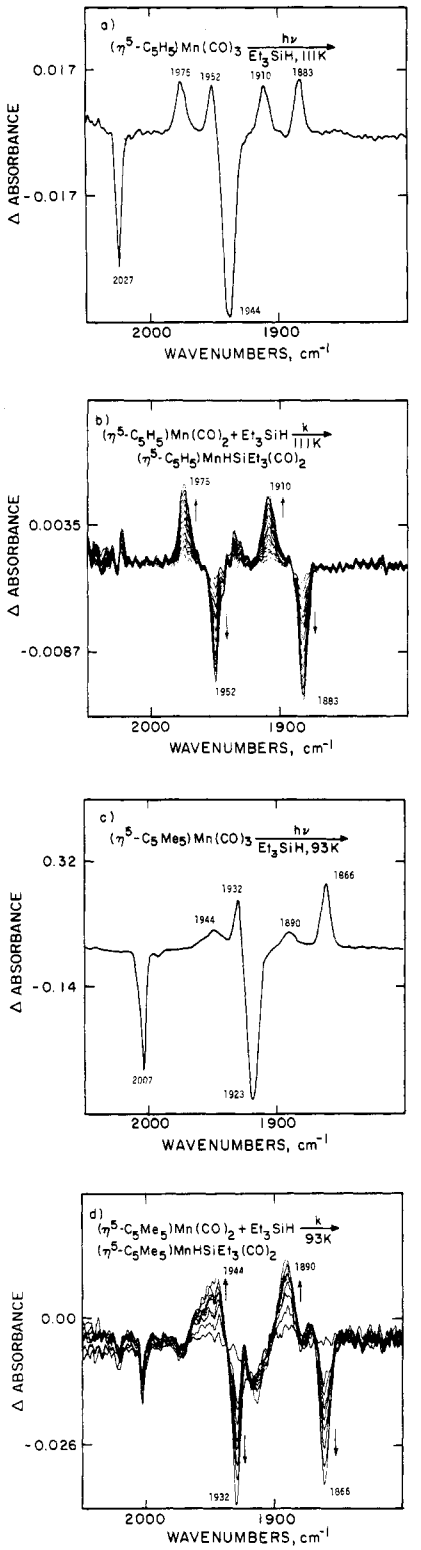

Figure 2. IR difference spectral changes accompanying (a) near-UV irradiation of $(\eta^5\text{-}C_5H_5)Mn(CO)_3$ for 30 s at 111 K to give a mixture of $(\eta^5\text{-}C_5H_5)Mn(CO)_2$ (1883, 1952 cm^{-1}) and $(\eta^5\text{-}C_5H_5)MnH(SiEt_3)(CO)_2$ (1910, 1975 cm^{-1}) and (b) the following thermal (dark) reaction of $(\eta^5\text{-}C_5H_5)Mn(CO)_2$ at times of 37, 77, 112, 162, 202, 242, 282, 362, 482, 622, 802, 1082, 1232, and 2122 s to give additional $(\eta^5\text{-}C_5H_5)MnH(SiEt_3)(CO)_2$. IR difference spectral changes accompanying (c) near-UV irradiation of $(\eta^5\text{-}C_5Me_5)Mn(CO)_3$ for 600 s at 93 K to give a mixture of $(\eta^5\text{-}C_5Me_5)Mn(CO)_2$ (1866, 1932 cm^{-1}) and $(\eta^5\text{-}C_5Me_5)MnH(SiEt_3)(CO)_2$ (1980, 1944 cm^{-1}) and (d) the following thermal dark reaction of $(\eta^5\text{-}C_5Me_5)Mn(CO)_2$ at times of 60, 980, 1640, 2240, 2900, 3500, 4040, 5060, and 5900 s to give additional $(\eta^5\text{-}C_5Me_5)MnH(SiEt_3)(CO)_2$. All data are for Et_3SiH as solvent.

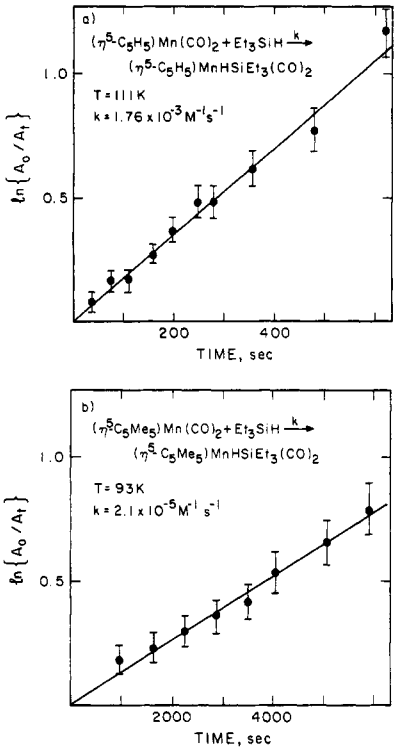

Figure 3. Plot of ln $\{A_0/A_t\}$ of the 16e species vs. time for (a) data from the experiment of Figure 2b and (b) data from the experiment of Figure 2d.

IR cell. This cell was then cooled to the desired temperature and photolyzed with a high-pressure Hg lamp. The IR spectrum was then obtained and typically showed a mixture of $(\eta^n\text{-}C_nR_n)M(CO)_3$, $(\eta^n\text{-}C_nR_n)M(CO)_2$, and $(\eta^n\text{-}C_nR_n)MH(SiR_3)(CO)_2$. The relative amounts of these species were dependent on the temperature, time of photolysis, and the particular chemical system. Subsequent FTIR spectra were obtained in the dark to determine the time dependence of the concentration of the 16e intermediate and the oxidative addition product. In each case the concentration of R_3SiH was in excess such that it did not vary significantly over the course of the reaction. The decay in concentration of $(\eta^n\text{-}C_nR_n)M(CO)_2$ (or increase in concentration of the $(\eta^n\text{-}C_nR_n)MH(SiR_3)(CO)_2$) was found to be first order in $(\eta^n\text{-}C_nR_n)M(CO)_2$. In each case the kinetic results were interpreted in terms of the second-order rate law given in eq 6.

$$\frac{-d[(\eta^n\text{-}C_nR_n)M(CO)_2]}{dt} = k[(\eta^n\text{-}C_nR_n)M(CO)_2][R_3SiH] \quad (6)$$

Figure 2 is a typical result obtained in the study of the reaction of $(\eta^5\text{-}C_5H_5)Mn(CO)_2$ with Et_3SiH. First a sample containing $(\eta^5\text{-}C_5H_5)Mn(CO)_3$ in Et_3SiH is cooled to 111 K and photolyzed. Upon photolysis there is a decrease in absorption bands at 1944 and 2027 cm^{-1} due to $(\eta^5\text{-}C_5H_5)Mn(CO)_3$ and appearance of absorption due to $(\eta^5\text{-}C_5H_5)Mn(CO)_2$ at 1883 and 1952 cm^{-1} and $(\eta^5\text{-}C_5H_5)MnH(SiEt_3)(CO)_2$ at 1910 and 1975 cm^{-1} (Figure 2a). At this point the sample is no longer irradiated, and the dark reaction, oxidative addition, producing more $(\eta^5\text{-}C_5H_5)MnH(SiEt_3)(CO)_2$ from the $(\eta^5\text{-}C_5H_5)Mn(CO)_2$ and Et_3SiH, is monitored (Figure 2b). Since the concentration of Et_3SiH is much greater than the 16e metal complex, the kinetics of the reaction are first-order in $(\eta^5\text{-}C_5H_5)Mn(CO)_2$. A plot of ln $[(\eta^5\text{-}C_5H_5)Mn(CO)_2]_{t=0}/[(\eta^5\text{-}C_5H_5)Mn(CO)_2]_t$ against time (Figure 3a) is, as expected, linear, and the slope divided by the concentration of Et_3SiH yields the

Table II. Rate Constants for Reaction of 16e $(\eta^n\text{-}C_nR_n)M(CO)_2$ Complexes with Et_3SiH[a]

$(\eta^n\text{-}C_nR_n)M(CO)_2$	$[HSiEt_3]$, M	T, K	k, M^{-1} s^{-1} (±10%)
$(\eta^4\text{-}C_4H_4)Fe(CO)_2$	6.3	118	3.65×10^{-5}
	6.3	123	1.12×10^{-4}
	6.3	128	6.82×10^{-4}
	6.3	133	2.7×10^{-3}
	6.3×10^{-2}	136[b]	7.4×10^{-3}
	6.3×10^{-3}	150[c]	6.0×10^{-1}
	1.9×10^{-2}	155[b]	1.4
	6.3×10^{-3}	157[b]	2.1
$(\eta^5\text{-}C_5H_5)Mn(CO)_2$	6.3	94	2.77×10^{-7}
	6.3	97	1.52×10^{-6}
	6.3	100	2.49×10^{-6}
	6.3	102	7.32×10^{-6}
	6.3	106	3.97×10^{-5}
	6.3	109	1.35×10^{-4}
	6.3	111	2.79×10^{-4}
	6.3	116	1.32×10^{-3}
	6.3	119	2.22×10^{-3}
	6.3	120	6.35×10^{-3}
	6.3×10^{-2}	140[b]	3.3×10^{-1}
	6.3×10^{-2}	142[b]	6.35×10^{-1}
$(\eta^5\text{-}C_5Me_5)Mn(CO)_2$	6.3	85	2.77×10^{-7}
	6.3	90	1.83×10^{-6}
	6.3	91	6.08×10^{-6}
	6.3	93	2.1×10^{-5}
	6.3	94	2.78×10^{-5}
	6.3	97	1.23×10^{-4}
	6.3	98	4.39×10^{-4}
	6.3	100	3.42×10^{-4}
	6.3	102	1.19×10^{-3}
	6.3	102	1.5×10^{-3}
	6.3	106	3.38×10^{-3}

[a] In Et_3SiH solvent unless otherwise noted. [b] In 3-methylpentane solvent. [c] In methylcyclohexane solvent.

Table III. Activation Parameters for Reaction of 16e $(\eta^n\text{-}C_nR_n)M(CO)_2$ with Et_3SiH

$(\eta^n\text{-}C_nR_n)M(CO)_2$	E_a, kJ mol^{-1}	$\Delta H^\ddagger$, kJ mol^{-1}	$\Delta S^\ddagger$, J mol^{-1} K^{-1}
$(\eta^4\text{-}C_4H_4)Fe(CO)_2$	46 ± 4	44 ± 4	47 ± 20
$(\eta^5\text{-}C_5H_5)Mn(CO)_2$	33 ± 4	30 ± 4	−28 ± 10
$(\eta^5\text{-}C_5Me_5)Mn(CO)_2$	33 ± 4	31 ± 4	16 ± 30

rate constant, k (2.8×10^{-4} M^{-1} s^{-1}), according to eq 6. A similar result is illustrated for the reaction of $(\eta^5\text{-}C_5Me_5)Mn(CO)_3$ with Et_3SiH at 93 K (Figure 2). The first step, photolysis, produces a mixture of $(\eta^5\text{-}C_5Me_5)Mn(CO)_2$, 1866 and 1932 cm^{-1}, and the oxidative addition adduct $(\eta^5\text{-}C_5Me_5)MnH(SiEt_3)(CO)_2$, 1890 and 1944 cm^{-1}, and loss of $(\eta^5\text{-}C_5Me_5)Mn(CO)_3$, 1923 and 2007 cm^{-1} (Figure 2c). The following thermal reaction, oxidative addition, is monitored as a function of time (Figure 2d), and a first order plot of ln $[(\eta^5\text{-}C_5Me_5)Mn(CO)_2]_{t=0}/[(\eta^5\text{-}C_5Me_5)Mn(CO)_2]_t$ vs. time is made (Figure 3b). The slope of this line divided by the concentration of Et_3SiH yields the rate constant, k (2.1×10^{-5} M^{-1} s^{-1}).

The calculated rate constants for reactions of Et_3SiH with $(\eta^n\text{-}C_nR_n)M(CO)_2$ vs. temperature are given in Table II. The assumption of a first-order dependance on Et_3SiH concentration is best shown to be justified by considering the Arrhenius plots for the reactions (Figure 4). The plots are linear despite a Et_3SiH concentratin variation of 2 orders of magnitude in the case of $(\eta^5\text{-}C_5H_5)Mn(CO)_2$. Similar results are obtained for $(\eta^4\text{-}C_4H_4)Fe(CO)_2$. Hence the assumption of an overall second-order rate law appears to be valid.

From the plots of Figure 3 and the data of Table II the activation parameters E_a, $\Delta H^\ddagger$, and $\Delta S^\ddagger$ were calculated[13] and are presented in Table III.[10] It is interesting to note that despite the broad range of conditions used (dilute

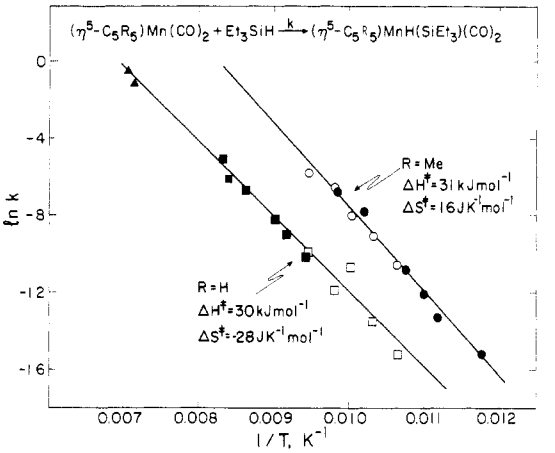

Figure 4. Arrhenius plot of ln k vs. $1/T$ for the oxidative addition reaction between Et_3SiH and $(\eta^5\text{-}C_5R_5)Mn(CO)_2$ where squares and triangles denote R = H and circles R = Me. The open circles and squares represent data that were obtained on a single sample containing both $(\eta^5\text{-}C_5H_5)Mn(CO)_3$ and $(\eta^5\text{-}C_5Me_5)Mn(CO)_2$, in order to make a direct comparison of the reactivity of these two species. The triangle points represent data for 6.3×10^{-2} M Et_3SiH in 3-methylpentane solvent, and all other data are for neat (6.3 M) Et_3SiH.

solution, neat liquid Et_3SiH, and Et_3SiH glass) all data points fit, within error, on one line for the plots of ln k vs. $1/T$ of $(\eta^4\text{-}C_4H_4)Fe(CO)_2$[10] and $(\eta^5\text{-}C_5H_5)Mn(CO)_2$. For the reaction of $(\eta^5\text{-}C_5Me_5Mn(CO)_2$, however, we were unable to follow the reaction in liquid hydrocarbon solvent or liquid Et_3SiH because reaction is too fast to measure at the temperatures where the solvents are fluid. For $(\eta^5\text{-}C_5H_5)Re(CO)_2$ a single measurement at low temperature indicated $t_{1/2} \approx 10$ min at 158 K in neat Et_3SiH corresponding to an approximate rate constant of 1.8×10^{-4} M^{-1} s^{-1}, i.e., slower than any of the other systems. Detailed studies for the Re system are complicated by the fact that back reaction according to eq 3 generally precludes oxidative addition at the temperatures where R_3SiH addition would be fast. Further, the photogeneration of the 16e Re species is relatively slow, preventing accumulation at temperatures where Et_3SiH reaction would be fast. Photolysis of $(\eta^6\text{-}C_6H_6)Cr(CO)_3$ in Et_3SiH 3-methylpentane containing Et_3SiH leads to direct conversion of $(\eta^6\text{-}C_6H_6)Cr(CO)_3$ to $(\eta^6\text{-}C_6H_6)CrH(SiEt_3)(CO)_2$ at 100K. In the absence of Et_3SiH no chemistry was observed upon photolysis. We attribute this to a low barrier for back reaction of $(\eta^6\text{-}C_6H_6)Cr(CO)_2$ with CO. It has been demonstrated that the primary photoprocess of $(\eta^6\text{-}C_6H_6)Cr(CO)_3$ at 4.2 K is indeed CO loss.[9] This indicates that under our conditions (~100 K) the barrier to reaction between CO or Et_3SiH and $(\eta^6\text{-}C_6H_6)Cr(CO)_2$ is sufficiently low that no unsaturated species is observed. This indicates that the reactivity of the Cr species with Et_3SiH is higher than that of the other 16e compounds studied. Attempts to study this reaction at lower temperature were complicated by crystallization of $(\eta^6\text{-}C_6H_6)Cr(CO)_3$ on cooling the glass (vide supra).

In order to study the effect of varying the silane, we chose to use the fragment $(\eta^5\text{-}C_5H_5)Mn(CO)_2$. The results were obtained by a series of competition studies using Et_3SiH as the standard. Typically a 3-methylpentane solution containing $(\eta^5\text{-}C_5H_5)Mn(CO)_3$, Et_3SiH, and R_3SiH was prepared and introduced into an IR cell. The sample was then photolyzed with a high intensity xenon flashlamp, and the relative amount of $(\eta^5\text{-}C_5H_5)MnH(SiEt_3)(CO)_2$ and $(\eta^5\text{-}C_5H_5)MnHSiR_3(CO)_2$ was determined by IR absorption. In order to minimize the effect of secondary photolysis, small conversions (<10%) of $(\eta^5\text{-}C_5H_5)Mn(CO)_3$ were used.

Relative rates of reaction at 298 K were obtained for the silanes Ph_3SiH, $EtMe_2SiH$, Et_3SiH, n-Pr_3SiH, and i-Pr_3SiH. For Ph_3SiH an additional competition experiment was done at 195 K, whereas for the trialkylsilanes a direct measurement of the rate constant for oxidative addition was made in the region of 100 K. IR data for the product species are included in Table I. From the kinetic and competition results (Table IV), the approximate activation parameters for the reaction of $(\eta^5\text{-}C_5H_5)Mn(CO)_2$ with the substituted silanes were calculated and are as follows: n-Pr_3SiH, $\Delta H^\ddagger = 30$ kJ mol^{-1} and $\Delta S^\ddagger = -31$ J K^{-1} mol^{-1}; i-Pr_3SiH, $\Delta H^\ddagger = 29$ kJ mol^{-1} and $\Delta S^\ddagger = -33$ J K^{-1} mol^{-1}; Ph_3SiH, $\Delta H^\ddagger = 28$ kJ mol^{-1}, and $\Delta S^\ddagger = -31$ J K^{-1} mol^{-1}; $EtMe_2SiH$, $\Delta H^\ddagger = 25$ kJ mol^{-1} and $\Delta S^\ddagger = -40$ J K^{-1} mol^{-1} (with estimated errors in the relative values of 1 kJ mol^{-1} in $\Delta H^\ddagger$ and 5 J K^{-1} mol^{-1} in $\Delta S^\ddagger$).

Discussion

The photochemical ejection of CO from $(\eta^n\text{-}C_nR_n)M(CO)_3$ to give coordinatively unsaturated species (eq 1) in low-temperature hydrocarbon glasses is consistent with previously observed photochemistry in Ar at 12 K.[9] The reaction of the 16e metal fragments with R_3SiH producing the oxidative addition products (eq 2) leads to net photosubstitution of CO by silane. This reactivity has been observed previously for the Mn and Cr complexes with Cl_3SiH and Ph_3SiH, and hence the reaction with trialkylsilanes is not surprising.[7a,d] For $(\eta^5\text{-}C_5H_5)Re(CO)_3$ photoreaction with trialkylsilanes has been observed previously.[7b-d] The trialkylsilane oxidative addition products appear to be less thermally stable than the Cl_3Si- and Ph_3Si- species reported previously. IR absorption spectra of all the R_3SiH addition products possess two, nearly equal intensity CO bands consistent with ~90° OC–M–CO angles.[14] Thus, in agreement with earlier studies, we formulate each $(\eta^n\text{-}C_nR_n)MH(SiR_3)(CO)_2$ complex as the cis isomer. This is consistent with the crystallographically determined structure of $(\eta^5\text{-}C_5H_4Me)MnH(SiMePhNp)(CO)_2$ which has a 91.4° OC–Mn–CO angle and $(\eta^5\text{-}C_5H_5)MnH(SiPh_3)(CO)_2$ with a 88.7° OC–Mn–CO angle (in the solid state) both prepared by photolysis of the appropriate tricarbonyl in the presence of silane.[15] It should be appreciated, however, that the oxidative addition of Si–H to the metal center is more or less complete depending on the particular system. There is considerable evidence that suggests that there is interaction between the H and Si in the oxidative addition product and that the bonding, in one extreme, can be viewed as a three-center (M, Si, H), two-electron system. Recent X-ray and neutron diffraction results and studies of ^{29}Si NMR to obtain the coupling constants J(SiMH) show that the extent to which the oxidative addition is complete is greater when there are electron-releasing ligands on M and/or highly electronegative substituents R on Si.[15c]

The formation of $(\eta^4\text{-}C_4H_4)FeH(SiEt_3)(CO)_2$ appears to be the first example of net CO loss followed by oxidative addition to the Fe species $(\eta^4\text{-}C_4H_4)Fe(CO)_3$. This result is not surprising since the Fe system is isoelectronic with the Mn, Re, and Cr species. In addition the electronically similar reaction of $(\eta^4\text{-}C_4Me_4)Fe(CO)_3$ with $OC(CF_3)_2$ forms $(\eta^4\text{-}Me_4C_4)Fe(OC(CF_3)_2)(CO)_2$.[16] As observed for the other complexes, the Fe adduct exhibits two equal intensity absorptions in the CO stretching region, consistent with a cis arrangement of the CO groups. The overall mechanism for the photochemical formation of $(\eta^n\text{-}C_nR_n)MH(SiR_3)(CO)_2$ is consistent with previous studies of CO loss from the Fe, Mn, and Cr[9] and was originally proposed by Jetz and Graham in the initial study of CO replacement by silane in $(\eta^5\text{-}C_5H_5)Mn(CO)_3$ and $(\eta^6\text{-}C_6H_6)Cr(CO)_3$.[7]

Table IV. Rate Constants for Reaction of $(\eta^5\text{-}C_5H_5)Mn(CO)_2$ with Silanes

silane	T, K	k, M^{-1} s^{-1} (±10%)[a]
Et_3SiH	298	9.8×10^5 [i]
	195	910[i]
	106	3.97×10^{-5} [ii]
Ph_3SiH	298	1.71×10^6 [iii]
	195	2611[iii]
i-Pr_3SiH	298	8.1×10^5 [iii]
	106	8.21×10^{-5} [ii]
$EtMe_2SiH$	298	1.76×10^6 [iii]
	106	3.3×10^{-3} [ii]
n-Pr_3SiH	298	7.41×10^5 [iii]
	108	7.34×10^{-5} [ii]

[a] Method of determination of k was the following: (i) extrapolation of low-temperature measurements, (ii) direct kinetic measurement, or (iii) competition experiments in which two different silanes (Et_3SiH as the standard) were present yielding relative rates. The competition experiments involved comparison with Et_3SiH whose rate at 195 and 298 K was obtained by extrapolation of data in Figure 4.

The Arrhenius plot for the reaction of $(\eta^4\text{-}C_4H_4)Fe(CO)_2$ or $(\eta^5\text{-}C_5H_5)Mn(CO)_2$ with Et_3SiH is linear although it contains data obtained in neat Et_3SiH solution, Et_3SiH glass, and dilute Et_3SiH in hydrocarbon solution (Figure 4). The self consistency of data for all three media indicates that data fit the activated complex theory equally well. One result of this is that the collisions between the unsaturated species and the Et_3SiH occur with the same temperature-dependent statistics in either solution or glass. This not only indicates similar vibrational but rotational motion in the two phases (the restricted translational motion is unimportant, as the glass consists of neat silane). The data are consistent with proposed glass structures having unrestricted rotational and vibrational motion but appear to be inconsistent with the proposed cluster model of glasses.[17] In the cluster model the glass structure contains areas of rigid clusters with fluidlike structure in between. If this were the case, we would expect the "cluster" areas to react much slower causing a significant deviation from fluid solution results, but Figure 4 shows that glasses and fluid solutions give data points that fall on the same linear Arrhenius plot.

The overall trend in reactivity at low temperature toward oxidative addition of R_3SiH is $(\eta^6\text{-}C_6H_6)Cr(CO)_2 > (\eta^5\text{-}C_5Me_5)Mn(CO)_2 > (\eta^5\text{-}C_5H_5)Mn(CO)_2 > (\eta^4\text{-}C_4H_4)Fe(CO)_2 > (\eta^5\text{-}C_5H_5)Re(CO)_2$. This reactivity trend appears to correlate with the electron density of the metal fragment as evidenced by the stretching frequencies; the more reactive fragments have the lower average CO stretching frequency. The Fe and Mn systems for which thermodynamic data were acquired, however, indicate that the reason for this reactivity trend is not simple. Values of $\Delta S^\ddagger$ and $\Delta H^\ddagger$ were calculated from activated complex theory and are given in Table IV. The activation enthalpies, $\Delta H^\ddagger$, are ordered $(\eta^4\text{-}C_4H_4)Fe(CO)_2 > (\eta^5\text{-}C_5H_5)Mn(CO)_2 \approx (\eta^5\text{-}C_5Me_5)Mn(CO)_2$ where the activation entropies, $\Delta S^\ddagger$, are ordered $(\eta^4\text{-}C_4H_4)Fe(CO)_2 > (\eta^5\text{-}C_5Me_5)Mn(CO)_2 > (\eta^5\text{-}C_5H_5)Mn(CO)_2$. The values of $\Delta S^\ddagger$ are not large and negative as might be expected for formation of an adduct, rather $\Delta S^\ddagger$ values vary from small and positive to small and negative. The reason for the

(16) Bond, A.; Green, M. *J. Chem. Soc., Chem. Commun.* **1971**, 12; *J. Chem. Soc., Dalton Trans.* **1972**, 763.

(17) Parsathasurathy, R.; Rad, K. J.; Rad, S. N. R. *Chem. Soc. Rev.* **1983**, *12*, 361.

positive $\Delta S^{\ddagger}$ appears to be solvation of the unsaturated species $(\eta^n\text{-}C_nH_n)M(CO)_2$. In addition to the $\Delta S^{\ddagger}$ values, the IR absorption frequencies of $(\eta^n\text{-}C_nR_n)M(CO)_2$ in Ar vs. organic glasses suggest a significant degree of solvent interaction. Despite the general trend of absorption moving to lower energy upon cooling, the unsaturated species in organic glasses at ~100 K absorb at lower energy than observed in Ar at ~12 K (Table I), indicating solvent interaction. The $\Delta S^{\ddagger}$ value then represents a compromise between the large positive value expected for solvent dissociation and the large negative value expected for Et_3SiH addition. That $\Delta S^{\ddagger}$ varies between positive and negative for the systems studied indicates a loosely bound silane molecule in the activated complex for the oxidative addition and/or very strong solvation of the $(\eta^n\text{-}C_nR_n)M(CO)_2$. Evidence concerning reaction according to eq 7

$$(\eta^5\text{-}C_5H_5)Mn(H)(SiPh_3)(CO)_2 + L \rightarrow (\eta^5\text{-}C_5H_5)Mn(CO)_2L + HSiPh_3 \quad (7)$$

tends to suggest some importance for a loosely bound silane in the transition state. The mechanism of this system was studied for both elimination of hydrido- and deuteriosilanes.[18] The data was found to be consistent with reductive elimination of silane followed by trapping of the 16e metal complex by a 2e donor ligand. The rate-determining step is then the reductive elimination of silane (eq 8), the reverse of the reaction studied here.

$$(\eta^5\text{-}C_5H_5)MnH(SiPh_3)(CO)_2 \rightarrow (\eta^5\text{-}C_5H_5)Mn(CO)_2 + HSiPh_3 \quad (8)$$

Considering the small magnitude of the observed kinetic isotope effect,[18] the authors argued that the activated complex consists of a very loosely bound R_3SiH, with a near complete Si–H bond. This is consistent with our $\Delta S^{\ddagger}$ values that can be thought of as representing the difference in order between a weakly solvated species and the activated complex. The entropy values observed are hence not inconsistent with rate-limiting Et_3SiH addition. Such hydrogen bonding to an unsaturated metal center has been suggested to be favorable by recent calculations.[19] Interestingly, it is the entropy term that is dominant in determining the higher reactivity of $(\eta^5\text{-}C_5Me_5)Mn(CO)_2$ compared to $(\eta^5\text{-}C_5H_5)Mn(CO)_2$ because $\Delta H^{\ddagger}$ for the reactions of Et_3SiH with either of these two complexes is the same within experimental error.

The activation parameters for reaction of $(\eta^5\text{-}C_5H_5)Mn(CO)_2$ with a variety of silanes were measured. For the trialkylsilanes Et_3SiH, $n\text{-}Pr_3SiH$, and $i\text{-}Pr_3SiH$ $\Delta H^{\ddagger}$ is about 30 kJ mol^{-1} and $\Delta S^{\ddagger}$ ~−30 J K^{-1} mol^{-1}. For the mixed trialkylsilane $EtMe_2SiH$ the activation paramaters were somewhat different with $\Delta H^{\ddagger}$ of 25 kJ mol^{-1} and $\Delta S^{\ddagger}$ of −40 J K^{-1} mol^{-1}. The activation paramaters for reaction of Ph_3SiH were $\Delta H^{\ddagger}$ = 28 kJ mol^{-1} and $\Delta S^{\ddagger}$ = −31 J K^{-1} mol^{-1}, very similar to the trialkylsilanes. The small variation in the activation paramaters is consistent with a loosely bound transition state in which reorganization of the solution contributes to the observed paramaters. In particular, the small negative values of $\Delta S^{\ddagger}$ can be compared with $\Delta S^{\ddagger}$ = −200 J K^{-1} mol^{-1} for reaction of $(EtO)_3SiH$ with $[(dppe)_2Ir][Ph_4B]$ ($\Delta H^{\ddagger}$ = 23 kJ mol^{-1}).[20] The higher reactivity of the $(\eta^n\text{-}C_nR_n)M(CO)_2$ species, compared to the Ir complex, is thus a result of the small values of $\Delta S^{\ddagger}$. The $\Delta H^{\ddagger}$ values vary only a small amount among the silanes reacted with $(\eta^5\text{-}C_5H_5)Mn(CO)_2$. This fact may indicate that $\Delta H^{\ddagger}$ reflects the activation enthalpy for dissociating the solvent from the site of ultimate oxidative addition. The data do not unambiguously rule out solvent dissociation as the step reflected in the $\Delta H^{\ddagger}$ values, but nonetheless the data for reaction of $(\eta^5\text{-}C_5H_5)Mn(CO)_2$ with the various silanes do appear to reveal experimentally significant differences among the silanes. The most sure conclusion, of course, is that $\Delta H^{\ddagger}$ for oxidative addition of the silane is rather modest. In view of the changes in the nature of the oxidative addition products with variation in the substituent R in R_3SiH,[15c] we intend to elaborate our studies to include examples of R groups that are more electronegative than the phenyl or alkyl groups used so far.

Acknowledgment. We thank the National Science Foundation for research support. R.H.H. acknowledges the Natural Sciences and Engineering Research Council of Canada for support in the form of a NATO postdoctoral fellowship, 1984–1986.

(18) Hart-Davis, A. J.; Graham, W. A. G. *J. Am. Chem. Soc.* **1971**, *93*, 4388.

(19) Saillard, J.-Y.; Hoffman, R. *J. Am. Chem. Soc.* **1984**, *106*, 2006.

(20) Harrod, J. F.; Smith, C. A. *J. Am. Chem. Soc.* **1970**, *92*, 2699.